

Role of Cooperative Hunting among Predators and Predator-Dependent Prey Refuge Behavior in a Predator-Prey Model*

Miqin Chen¹ and Wensheng Yang^{1,2,†}

Abstract The investigation of predator cooperative hunting and prey refuge is crucial for understanding ecological dynamics. In recent years, the role of cooperative hunting or prey refuge in predator-prey systems has received much attention from researchers. However, the study on the combined effects of predator cooperation and predator-dependent prey refuge in the predation system has not yet been investigated. Therefore, in this paper, we propose a prey-predator model with both the factors of predator-dependent prey refuge and cooperative hunting. The positivity and boundedness of the system's solutions are investigated, followed by the existence and local stability of the equilibrium points. Sufficient conditions for the existence of Hopf bifurcation of the system are obtained. The direction of Hopf bifurcation in the system is investigated by using the center manifold theorem and normal form method. From the analysis of the model, we find that the dependence coefficient m of the prey refuge ratio on the number of predators may be responsible for the stability of the system. The results also indicate that suitable competition coefficients s and cooperative hunting coefficients α between predators may enable the species to coexist in the long run. Furthermore, we observe two limit cycles of the system when the parameters satisfy certain conditions. Finally, the dynamical behavior of the model is performed through intriguing numerical simulations.

Keywords Predator-prey model, hunting cooperation, predator-dependent prey refuge, Hopf bifurcation

MSC(2010) 34D23, 92D25, 92D45.

1. Introduction

The predator-prey model is an important mathematical model in population dynamics and an important study branch in the field of biomathematics. Understanding the regulating mechanism in the process of predation and then accurately predicting and estimating the population size of predator and prey is enhanced by studying the

[†]the corresponding author.

Email address: 2050622812@qq.com (M. Chen), ywensheng@126.com (W. Yang)

¹School of Mathematics and Statistics, Fujian Normal University, Fuzhou, Fujian 350117, China

²FJKLMAA and Center for Applied Mathematics of Fujian province (FJNU), Fuzhou, Fujian 350117, China

*The authors were supported by the Natural Science Foundation of China (11672074), the Natural Science Foundation of Fujian Province (2022J01192).

various features of predator-prey models. When investigating various predator-prey models in recent years, many scholars have taken the cooperative hunting behavior of predator populations into consideration [1–5].

Cooperative hunting means that predator groups work together to improve the efficacy of foraging. For example, cooperative hunting exists in crocodiles [6], lions [7], wolves [8], spiders [9], eagles [10], ants [11] and other species. To more adequately describe the phenomenon of cooperative hunting across predator populations, Cosner et al. [12] proposed a functional response in 1999 in which a predator feeds in a spatially linear pattern and the predators congregate when they encounter a group of prey. In 2010, Berec [13] used ordinary differential equations to simulate a predator-prey model with Holling-II functional response to explain the foraging facilitation between predators and discussed the influence of different intensities of predator interference on the dynamics of the predator-prey model. Following that, in 2017, Alves and Hilker [14] argued that cooperative hunting has an impact on predator population attack rates and that it is necessary to add a cooperative item to predator population attack rates, and proposed the following functional response

$$\Phi(x, y) = (l + \alpha y)x,$$

where x and y denote prey and predator, respectively; both l and α are positive model parameters. l is the attack rate of a predator on prey, α is the cooperative hunting efficiency of a predator, and αy is the cooperative term. Therefore, they developed the following model of cooperative hunting with the Holling-I functional response

$$\begin{cases} \frac{dx}{dt} = rx \left(1 - \frac{x}{k}\right) - (l + \alpha y)xy, \\ \frac{dy}{dt} = e(l + \alpha y)xy - dy, \end{cases} \quad (1.1)$$

where r is the intrinsic growth rate of prey per capita, k is the carrying capacity of prey, e is the conversion efficiency, and d is the predators' per capita mortality rate. All parameters are positive. There have been many results in the discussion of model (1.1). For instance, Zhang et al. [15] investigated the existence and stability of the positive equilibrium point as well as the optimal control problem after introducing the Allee effect into the model (1.1). Pal et al. [16] considered the impact of hunting cooperation and the fear factor on the dynamics of the predator-prey model by incorporating a fear factor into the model (1.1). Halder et al. [17] investigated that cooperative hunting produced both fear and Allee effect under Holling type I and Holling type II functional response. Recently, Thirthar et al. [18] examined the effect of fear in a predator-prey model with additional food, prey refuge, and harvesting by the super predator.

In an ecosystem, fear induced refuge is another fascinating and critical factor that is acquired by prey. It plays an important role in balancing predator-prey interactions. Thus, for an ecosystem, the concept of refuge is worthy of investigation [19]. For modeling purposes, two types of refuges are commonly used by many researchers. The quantity of prey in cover x_r is proportional to prey density x , that is, $x_r = \theta x$. The other one, for which the refuge population is a fixed quantity $x_r = \theta$. Ruxton [20] considered $x_r = \theta xy$, where y is predator density. In the present article, we are interested in investigating the situation where prey in the refuge is related to the number of predators which is $x_r = \theta(1 - \frac{1}{1+my})x = \frac{\theta my}{1+my}x$,

where θ is the prey refuge coefficient and m indicates that the prey refuge ratio is a coefficient dependent on the number of predators. Further, x_r is monotonically increasing with respect to y ; if $y = 0$, then $x_r = 0$, which means if the predator does not exist, the prey refuge population is zero; if y tends to infinity, then this translates into a ratio refuge, which is a common type. Thus, the number of prey available to the predator is $x - x_r = \frac{1+(1-\theta)my}{1+my}x$.

Inspired by the above work, in this paper we will consider prey refuge based on the model (1.1), where the number of prey refuge depends on the number of predators. Compared to model (1.1), we consider that this predator-dependent refuge will be more ecologically meaningful than proportional or constant refuge. We will consider the following model

$$\begin{cases} \frac{dx}{dt} = rx(1 - \frac{x}{k}) - (l + \alpha y) \frac{1 + (1 - \theta)my}{1 + my} xy, \\ \frac{dy}{dt} = e(l + \alpha y) \frac{1 + (1 - \theta)my}{1 + my} xy - (d + sy)y, \end{cases} \quad (1.2)$$

with initial conditions:

$$x(0) \geq 0, y(0) \geq 0,$$

where $x(t)$ and $y(t)$ denote the number of prey and predator populations respectively, at any time t . And the biological significance of other parameters are described in Table 1. For ecological realism, we restrict θ such that $(1 - \theta) > 0$.

Table 1. Parameters and their descriptions used in system (1.2).

Parameters	Description
r	Intrinsic prey growth rate
k	Environmental intake capacity
l	Attack rate per predator and prey
α	Predator hunting cooperation
θ	Prey refuge coefficient
m	Prey refuge rate depends on the number of predator
e	Conversion factor
d	Natural mortality rate of the predator
s	Intraspecific competition rate of predator

The rest of the paper is organized as follows. In Section 2, we discuss the boundedness and positivity of the solution of the system (1.2) and investigate the existence of the equilibrium points. In Section 3, we determine the local stability of each equilibrium point. In Section 4, we establish criteria for local and global bifurcations using center-manifold and normal-form theory. All our analytical results are verified numerically using MATLAB in Section 5. Finally, based on the above discussion, we give some conclusions in Section 6.

2. Preliminary analysis

2.1. Positivity and boundedness of the solution

In this subsection, we shall first show the positivity and bounds solutions to the system (1.2), which are vital for the biological understanding of the system and the subsequent analysis.

Lemma 2.1. *All the solutions of system (1.2), which start in R_+^2 , are always positive and bounded.*

Proof. Firstly, we want to prove that $(x(t), y(t)) \in R_+^2$ for all $t \in [0, +\infty)$. For system (1.2) with initial conditions $x(0) > 0$, $y(0) > 0$, we have

$$\begin{aligned} x(t) &= x(0) \exp \left\{ \int_0^t \left[r \left(1 - \frac{x(s)}{k} \right) - (l + \alpha y(s)) \frac{1 + (1 - \theta)my(s)}{1 + my(s)} y(s) \right] ds \right\}, \\ y(t) &= y(0) \exp \left\{ \int_0^t \left[e(l + \alpha y(s)) \frac{1 + (1 - \theta)my(s)}{1 + my(s)} x(s) - (d + sy(s)) \right] ds \right\}, \end{aligned} \quad (2.1)$$

which shows that all the solutions of system (1.2) are always positive for all $t \geq 0$.

Secondly, we will prove the boundedness of the solution. Let $x(t)$, $y(t)$ be the solution of the system (1.2), and define the function $W(t) = x(t) + \frac{1}{e}y(t)$ and $\eta > 0$ be some constant. Then

$$\begin{aligned} \frac{dW}{dt} &= \frac{dx}{dt} + \frac{1}{e} \frac{dy}{dt}, \\ &= rx \left(1 - \frac{x}{k} \right) - \frac{1}{e} (d + sy)y. \end{aligned}$$

Next,

$$\begin{aligned} \frac{dW}{dt} + \eta W &= rx \left(1 - \frac{x}{k} \right) - \frac{1}{e} (d + sy)y + \eta x + \frac{1}{e} \eta y, \\ &= x \left(r \left(1 - \frac{x}{k} \right) + \eta \right) + \frac{1}{e} (\eta - (d + sy))y, \\ &\leq x \left(r \left(1 - \frac{x}{k} \right) + \eta \right) + \frac{1}{e} (\eta - d)y. \end{aligned}$$

Now, we choose $\eta \in (0, d)$. The maximum value of $x \left(r \left(1 - \frac{x}{k} \right) + \eta \right)$ is $\frac{(\eta+r)^2 k}{4r}$. Then, we have

$$\frac{dW}{dt} + \eta W \leq \frac{(\eta+r)^2 k}{4r} = \beta.$$

Therefore, applying differential inequality, we obtain

$$0 \leq W(t) \leq \frac{\beta}{\eta} + W(x(0), y(0))e^{\eta t}.$$

Thus, all solutions of system (1.2) enter into the region $D = \{(x, y) : 0 \leq W(x, y) \leq \frac{\beta}{\eta}\}$. This shows that every solution of the system (1.2) is bounded. \square

2.2. The existence of equilibria

- (i) The trivial equilibrium $E_0(0, 0)$ always exists.
- (ii) The predator free equilibrium $E_1(k, 0)$ is always feasible.
- (iii) Now we analyze the existence of the positive equilibrium $E^*(x^*, y^*)$, where the expressions of x^* , y^* can be obtained by solving the following equations

$$\begin{aligned} r\left(1 - \frac{x^*}{k}\right) - (l + \alpha y^*) \frac{1 + (1 - \theta)my^*}{1 + my^*} y^* &= 0, \\ e(l + \alpha y^*) \frac{1 + (1 - \theta)my^*}{1 + my^*} x^* - (d + sy^*) &= 0. \end{aligned} \quad (2.2)$$

From (2.2), we solve that

$$x^* = \frac{(d + sy^*)(1 + my^*)}{e(l + \alpha y^*)(1 + (1 - \theta)my^*)} > 0,$$

and y^* is the root of the equation

$$a_1 y^{*5} + a_2 y^{*4} + a_3 y^{*3} + a_4 y^{*2} + a_5 y^* + a_6 = 0, \quad (2.3)$$

where

$$\begin{aligned} a_1 &= e k \alpha^2 m^2 (\theta - 1)^2, \\ a_2 &= 2 e k \alpha^2 m (1 - \theta) + 2 e k l \alpha m^2 (\theta - 1)^2, \\ a_3 &= e k \alpha^2 + e k \alpha m (4l - r m) (1 - \theta) + e k l^2 m^2 (\theta - 1)^2 + r s m^2, \\ a_4 &= d m^2 r + 2 m r s + 2 e k l^2 m (1 - \theta) + \alpha e k m r (\theta - 2) + e k l m^2 r (1 + \theta) + 2 \alpha e k l, \\ a_5 &= r s + 2 d m r + e k l^2 - \alpha e k r + e k l m r (\theta - 2), \\ a_6 &= r (d - e k l). \end{aligned}$$

3. Stability analysis

We compute the Jacobian matrix for system (1.2) to investigate the local stability of equilibria whenever they exist. $J(x, y)$ of system (1.2) at any point (x, y) is given by

$$J(x, y) = \begin{pmatrix} J_{11} & J_{12} \\ J_{21} & J_{22} \end{pmatrix}, \quad (3.1)$$

where

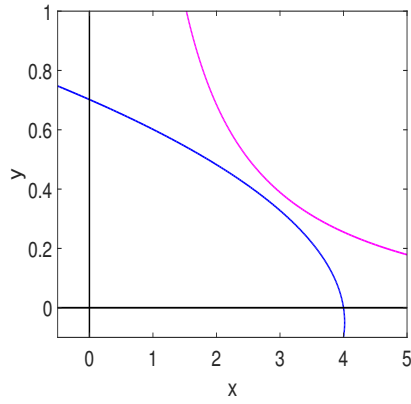


Figure 1. *
 $\alpha = 0.5, elk < d$

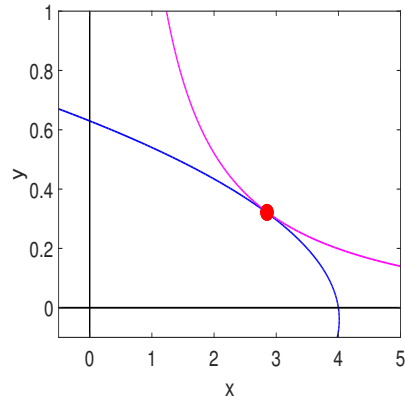


Figure 2. *
 $\alpha = 0.64, elk < d$

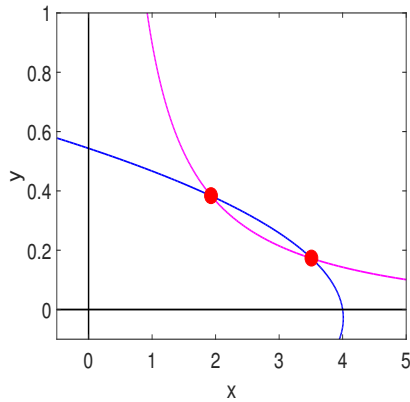


Figure 3. *
 $\alpha = 0.86, elk < d$

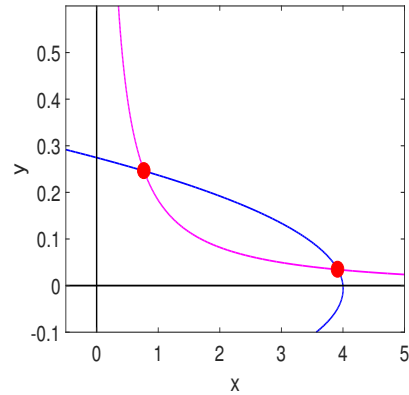


Figure 4. *
 $\alpha = 3.54, elk < d$

Figure 5. The number of possible positive internal equilibrium points for different values of hunting cooperation α ; (a) the system (1.2) has no positive equilibrium point for $\alpha = 0.5$; (b) there exists only one equilibrium point for $\alpha = 0.64$; when α continues to increase, the graphs (c) and (d) show that the system (1.2) will have two equilibrium points. The other parameters are as follows: $r = 0.28$, $k = 4$, $l = 0.05$, $\theta = 0.26$, $m = 0.03$, $e = 0.18$, $d = 0.12$, $s = 0.03$.

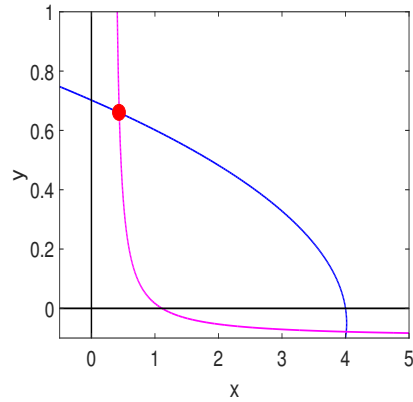


Figure 6. *
 $\alpha = 0.5, elk > d$

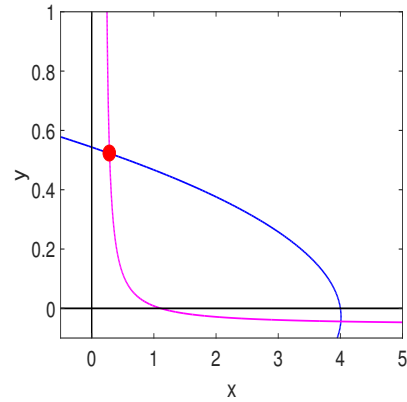


Figure 7. *
 $\alpha = 0.64, elk > d$

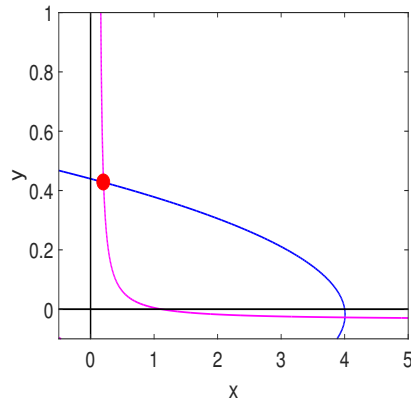


Figure 8. *
 $\alpha = 0.86, elk > d$

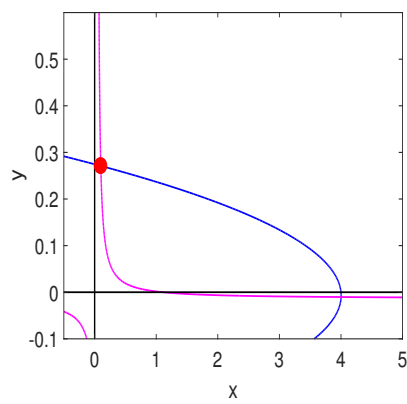


Figure 9. *
 $\alpha = 3.54, elk > d$

Figure 10. The number of possible positive internal equilibrium points for different values of hunting cooperation α . No matter what value α takes, the system (1.2) has only one positive equilibrium point when the parameter satisfies $elk > d$. The other parameters are as follows: $r = 0.28$, $k = 4$, $l = 0.05$, $\theta = 0.26$, $m = 0.03$, $e = 0.18$, $d = 0.01$, $s = 0.03$.

$$\begin{aligned}
J_{11} &= r\left(1 - \frac{2x}{k}\right) - (l + \alpha y) \frac{1 + (1 - \theta)my}{1 + my} y, \\
J_{12} &= -\frac{\alpha xy(1 + (1 - \theta)my)}{1 + my} - \frac{(l + \alpha y)(1 - \theta)mxy}{1 + my} - \frac{x(l + \alpha y)(1 + my(1 - \theta))}{1 + my} \\
&\quad + \frac{mxy(l + \alpha y)(1 + my(1 - \theta))}{(1 + my)^2}, \\
J_{21} &= e(l + \alpha y) \frac{1 + (1 - \theta)my}{1 + my} y, \\
J_{22} &= e\alpha \frac{(1 + (1 - \theta)my)xy}{1 + my} + \frac{ex(l + \alpha y)(1 + 2my(1 - \theta))}{1 + my} \\
&\quad - \frac{e(l + \alpha y)(1 + (1 - \theta)my)mxy}{(1 + my)^2} - d - 2sy.
\end{aligned}$$

The local stability is analyzed below by calculating the Jacobian matrix corresponding to each equilibrium point.

Accordingly, for the trivial equilibrium point E_0 , the Jacobian matrix takes the form as

$$J(E_0) = \begin{pmatrix} r & 0 \\ 0 & -d \end{pmatrix}. \quad (3.2)$$

The eigenvalues of $J(E_0)$ are r and $-d$. Therefore, E_0 is a saddle point. So we have the following theorem.

Theorem 3.1. *The trivial equilibrium E_0 is always unstable.*

Next, the Jacobian matrix of E_1 is given by

$$J(E_1) = \begin{pmatrix} -r & kl \\ 0 & elk - d \end{pmatrix}. \quad (3.3)$$

The eigenvalues of the Jacobian matrix at E_1 are $-r$ and $elk - d$. Since all parameter values are non-negative, the trivial equilibrium E_1 is stable if $elk < d$ and unstable if $elk > d$. Based on the above discussion, we have the following Theorem.

Theorem 3.2. *Predator-free equilibrium point E_1 is locally asymptotically stable if $elk < d$; otherwise, it is a saddle point if $elk > d$.*

Evaluating the Jacobian matrix of the model system (1.2) at the interior equilibrium point $E^* = (x^*, y^*)$, we have

$$J(E^*) = \begin{pmatrix} J_{11}^* & J_{12}^* \\ J_{21}^* & J_{22}^* \end{pmatrix},$$

where

$$\begin{aligned}
J_{11}^* &= -\frac{rx^*}{k}, \\
J_{12}^* &= -\frac{\alpha x^* y^* (1 + (1 - \theta)my^*)}{1 + my^*} - \frac{(l + \alpha y^*)(1 - \theta)mx^* y^*}{1 + my^*} - \frac{d + sy^*}{e} \\
&\quad + \frac{mx^* y^* (l + \alpha y^*)(1 + my^*(1 - \theta))}{(1 + my^*)^2}, \\
J_{21}^* &= \frac{d + sy^*}{x^*}, \\
J_{22}^* &= \frac{(d + sy^*)\alpha y^*}{l + \alpha y^*} + \frac{ex^*(l + \alpha y^*)(1 + 2my^*(1 - \theta))}{1 + my^*} \\
&\quad - \frac{e(l + \alpha y^*)(1 + (1 - \theta)my^*)mx^* y^*}{(1 + my^*)^2} - d - 2sy^*.
\end{aligned}$$

The characteristic equation around E^* is $\lambda^2 - \text{Tr}(J(E^*))\lambda + \text{Det}(J(E^*)) = 0$, where

$$\begin{aligned}
\text{Tr}(J(E^*)) &= J_{11}^* + J_{22}^*, \\
\text{Det}(J(E^*)) &= J_{11}^* J_{22}^* - J_{12}^* J_{21}^*.
\end{aligned} \tag{3.4}$$

Now, if $\text{Tr}(J(E^*)) < 0$ and $\text{Det}(J(E^*)) > 0$, by using the Routh-Hurwitz criterion, all the eigenvalues of $J(E^*)$ have a negative real part. According to the above discussion, we can obtain the following theorem.

Theorem 3.3. *The positive equilibrium point E^* is always locally asymptotically stable if $\text{Tr}(J(E^*)) < 0$ and $\text{Det}(J(E^*)) > 0$.*

4. Bifurcation analysis

Now, in this section, we consider the bifurcation of the system (1.2) when there exists a positive equilibrium point E^* . Then, we focus on the conditions for the existence of Hopf bifurcation in the system (1.2) and the direction of the Hopf bifurcation of the system (1.2) occurring at the positive equilibrium point E^* .

Define $\mu_1 = \text{Tr}(J(E^*))$, $\mu_2 = \text{Det}(J(E^*))$. Select m as the hopf bifurcation parameter if there exists $m = m_{hb}$, such that $H_1 : \text{tr}(J(E^*))|_{m=m_{hb}} = 0$, $\text{det}(J(E^*))|_{m=m_{hb}} > 0$ and $2\mu'_1\mu_2 + \mu_1\mu'_2 \neq 0$ holds, where μ'_1 and μ'_2 denote the derivatives of μ_1 and μ_2 with respect to m , respectively.

Theorem 4.1. *Assume that condition H_1 holds. When $m = m_{hb}$, the system (1.2) undergoes a Hopf bifurcation at the positive equilibrium point E^* .*

Proof. The Jacobian the characteristic equationmatrix at the positive equilibrium point E^* corresponds to the following characteristic equations

$$\lambda^2 - \mu_1\lambda + \mu_2 = 0. \tag{4.1}$$

When $m = m_{hb}$, $\mu_1 = 0$, the characteristic equation (4.1) can be described as

$$\lambda^2 + \mu_2 = 0, \tag{4.2}$$

then, equation (4.2) will have a pair of purely imaginary roots as $\lambda_1 = i\sqrt{\mu_2}$, $\lambda_2 = -i\sqrt{\mu_2}$. Next, differentiating the characteristic equation (4.1) with respect to m , we will obtain

$$2\lambda \frac{d\lambda}{dm} - \lambda\mu'_1 - \frac{d\lambda}{dm}\mu_1 + \mu'_2 = 0. \quad (4.3)$$

Rectifying the equation (4.3) we can get

$$\frac{d\lambda}{dm} = \frac{\lambda\mu'_1 - \mu'_2}{2\lambda - \mu_1}, \quad (4.4)$$

then,

$$\left. \frac{d\lambda}{dm} \right|_{\lambda=i\sqrt{\mu_2}} = \frac{2\mu'_1\mu_2 + \mu_1\mu'_2}{4\mu_2 + \mu_1^2} + i \left[\frac{2\sqrt{\mu_2}\mu'_2 - \mu_1\sqrt{\mu_2}\mu'_2}{4\mu_2 + \mu_1^2} \right]. \quad (4.5)$$

Consequently,

$$\operatorname{Re} \left(\frac{d\lambda}{dm} \right) \Big|_{\lambda=i\sqrt{\mu_2}} = \frac{2\mu'_1\mu_2 + \mu_1\mu'_2}{4\mu_2 + \mu_1^2} \neq 0. \quad (4.6)$$

Thus, we know that system (1.2) undergoes a Hopf-bifurcation at E^* as s passes through value m_{hb} . \square

Next, we calculate the first Lyapunov number σ at the system (1.2) positive equilibrium point E^* to further explore the nature of the limit cycle.

Let $u = x - x^*$, $v = y - y^*$. The system (1.2) reduces to

$$\begin{aligned} \frac{du}{dt} &= a_{10}u + a_{01}v + a_{11}uv + a_{20}u^2 + a_{02}v^2 + a_{30}u^3 + a_{21}u^2v + a_{12}uv^2 + a_{03}v^3 \\ &\quad + P(u, v), \\ \frac{dv}{dt} &= b_{10}u + b_{01}v + b_{11}uv + b_{20}u^2 + b_{02}v^2 + b_{30}u^3 + b_{21}u^2v + b_{12}uv^2 + b_{03}v^3 \\ &\quad + Q(u, v), \end{aligned}$$

where

$$\begin{aligned} a_{10} &= -\frac{rx^*}{k}, \\ a_{01} &= -\alpha y^* \frac{m + sy^*}{e(l + \alpha y^*)} - \frac{(m + sy^*)(1 - \theta)my^*}{e(1 + (1 - \theta)my^*)} - \frac{m_sy^*}{e} + \frac{(m + sy^*)my^*}{e(1 + my^*)}, \\ a_{20} &= -\frac{r}{2k}, \quad a_{11} = 0, \\ a_{02} &= \frac{\alpha(l + \alpha y^*)(m + 2sy^*) - \alpha^2(my^* + sy^{*2})}{2e(l + \alpha y^*)^2} \\ &\quad - \frac{(1 - \theta)m(m + 2sy^*)(1 + (1 - \theta)my^*) - (1 - \theta)^2m^2y^*(m + sy^*)}{2e(1 + (1 - \theta)my^*)^2} \\ &\quad - \frac{s}{2e} - \frac{(1 + my^*)(m + 2sy^*)m - m^2(my^* + sy^{*2})}{2e(1 + my^*)^2}, \end{aligned}$$

$$\begin{aligned}
a_{30} &= 0, & a_{21} &= 0, & a_{12} &= 0, \\
a_{03} &= \frac{2\alpha s}{12e(l + \alpha y^*) - \frac{\alpha l(m + sy^*)}{12e^2(l + \alpha y^*)^4}} - \frac{2ms(1 - \theta)}{12e(1 + (1 - \theta)my^*)} \\
&\quad - \frac{2m^2(1 - \theta)^2(m + 2sy^* + msy^{*2})}{12e(1 + (1 - \theta)my^*)^3} + \frac{2ms}{12e(1 + my^*)} \\
&\quad - \frac{2m^2(m + 2sy^* + msy^{*2})}{12e(1 + my^*)^3}, \\
b_{10} &= \frac{(m + sy^*)y^*}{x^*}, \\
b_{01} &= \frac{(m + sy^*)}{l + \alpha y^*} + \frac{(m + sy^*)(x^* + 2(1 - \theta))}{(1 + (1 - \theta)my^*)x^*} - \frac{(m + sy^*)my^*}{1 + my^*} - d - 2sy^*, \\
b_{20} &= \frac{-(m + sy^*)y^*}{2x^{*2}}, b_{11} = \frac{m + 2sy^*}{x}, \\
b_{02} &= \frac{m\alpha(1 + 2sy^*)}{2(l + \alpha y^*)} - \frac{(m + sy^*)\alpha^2 y^*}{2(l + \alpha y^*)^2} + \frac{s(x^* + 4(1 - \theta)mx^*y^*) + 2(1 - \theta)m^2x^*}{2(1 + (1 - \theta)my^*)x^*} \\
&\quad - \frac{m(1 - \theta)(m + 2sy^*)(x^* + 2(1 - \theta)mx^*y^*)}{2(1 + (1 - \theta)my^*)^2x^*} - \frac{m^2(1 + 2sy^*)}{2(1 + my^*)} \\
&\quad + \frac{m^2y^*(m + sy^*)}{2(1 + my^*)^2} - 4s, \\
b_{30} &= \frac{(m + sy^*)y^*}{6x^{*3}}, b_{21} = \frac{-(m + 2sy^*)}{4x^{*2}}, b_{12} = \frac{s}{x^*}, \\
b_{03} &= \frac{2m\alpha s}{12(l + \alpha y^*)} - \frac{m\alpha^2(1 + 2sy^*)}{12(l + \alpha y^*)^2} + \frac{2(m + sy^*)\alpha^3 y^*(1 + (1 - \theta)my^*)^2x^*}{12(l + \alpha y^*)^3} \\
&\quad + \frac{4(1 - \theta)smx^*}{12(1 + (1 - \theta)my^*)x^*} \\
&\quad - \frac{m(1 - \theta)(sx^* + 2(1 - \theta)msx^*y^*) + 2(1 - \theta)mx^*(m + sy^*)}{12(1 + (1 - \theta)my^*)^2x^*} \\
&\quad + \frac{2m^2(1 - \theta)^2(m + sy^*)(x^* + 2(1 - \theta)mx^*y^*)}{12(1 + (1 - \theta)my^*)^3x^*} \\
&\quad - \frac{m^2(2s - m)}{12(1 + my^*)^2} + \frac{2m^3y^*(m + sy^*)}{12(1 + my^*)^3}, \\
P(u, v) &= \sum_{i+j=4}^{+\infty} a_{ij}u^i v^j, & Q(u, v) &= \sum_{i+j=4}^{+\infty} b_{ij}^4 u^i v^j.
\end{aligned}$$

Hence the first Lyapunov number σ for a planar system is given by

$$\begin{aligned}
\sigma &= -\frac{3\pi}{2a_{01}\Delta^{\frac{3}{2}}} \{ [a_{10}b_{10}(a_{11}^2 + a_{11}b_{02} + a_{02}b_{11}) + a_{10}a_{01}(b_{11}^2 + a_{20}b_{11} + a_{11}b_{02}) \\
&\quad + b_{10}^2(a_{11}a_{02} + 2a_{02}b_{02}) - 2a_{10}b_{10}(b_{02}^2 - a_{20}a_{02}) - 2a_{10}a_{01}(a_{20}^2 - b_{20}b_{02}) \\
&\quad - a_{01}^2(2a_{20}b_{20} + b_{11}b_{20}) + (a_{01}b_{10} - 2a_{10}^2)(b_{11}b_{02} - a_{11}a_{20})] \\
&\quad - (a_{10}^2 + a_{01}b_{10})[3(b_{10}b_{03} - a_{01}a_{30}) + 2a_{10}(a_{21} + b_{12}) + (b_{10}a_{21} - a_{01}b_{21})] \},
\end{aligned}$$

where $\Delta = a_{10}b_{01} - a_{01}b_{10}$.

The periodic solution is subcritical or supercritical in nature if the value of $\sigma > 0$ or $\sigma < 0$, respectively.

5. Numerical simulations

In this section, we will verify the theoretical results obtained in the previous sections through Matlab numerical simulations. In order to get a more comprehensive understanding of the existence and stability of the equilibrium point of the system (1.2). We divide the parameter selection into two categories, i.e., parameter conditions satisfying $elk < d$ or $elk > d$. First, we take into consideration the following parametric values:

$$r = 0.28, k = 4, l = 0.05, \theta = 0.26, m = 0.03, e = 0.18, d = 0.12, s = 0.03, \quad (5.1)$$

and the stability of the system (1.2) at each positive equilibrium point is shown in Figure 3. Here, we choose a different predator hunting coefficient α to analyze, and we find that in Figure 3(a), two nullclines intersect at the unique positive equilibrium point $E^{1*} = (2.7532, 0.33275)$, and the eigenvalues at E^{1*} are -0.062588 and -0.035185 . Obviously, E^{1*} is a nodal sink. In this case, both species may survive in a coexisting steady state. For $\alpha = 0.68$, both prey and predator nullclines intersect at two positive equilibrium points in Figure 3(b). The eigenvalues of the equilibrium point $E_2^{2*} = (2.4413, 0.36606)$ are $-0.036582 + 0.09008i$ and $-0.036582 - 0.09008i$. The complex eigenvalues have negative real parts. Thus, the positive equilibrium point E_2^{2*} is locally asymptotically stable. On the other hand, the eigenvalues of the equilibrium point $E_2^{1*} = (3.1998, 0.25288)$ are $(-0.17655, 0.043673)$, therefore, E_2^{1*} is a saddle point. In Figure 3(c), $\alpha = 1$, and it is found that $E_2^{2*} = (1.7164, 0.37618)$ is still a locally asymptotically stable point. When α is increased continuously to 1.5, a limit cycle for the system (1.2) appears in Figure 3(d). In Figure 3(e) and Figure 3(f), there is a spiral source at E_2^{2*} . In addition, in Figure 3, the boundary equilibrium point E_1 is always locally asymptotically stable.

Then, we select a set of parameters to satisfy $elk < d$, as follows:

$$r = 0.28, k = 4, l = 0.05, \theta = 0.26, m = 0.03, e = 0.18, d = 0.01, s = 0.03, \quad (5.2)$$

with initial condition $(0.3, 0.6)$. It is clear to see that this set of parameters satisfies $elk > d$. In Figure 4(a), it is found that the eigenvalues of the equilibrium point $E_1^* = (0.28679, 0.52256)$ are $-0.0063774 + 0.11165i$ and $-0.0063774 - 0.11165i$. Thus, the interior equilibrium point E_1^* is a spiral sink. In Figure 4(b), for $\alpha = 3.54$, it is noted that two limit cycles appear in the system. In addition, the boundary equilibrium point $E_1 = (4, 0)$ is always a saddle point.

After examining the stability of the equilibrium point, time series, phase diagram, and Hopf bifurcation are used to undertake a temporal study of the system (1.2). In Figure 5, when α is between 0.5 and 3.54, the increase in predator-prey cooperation coefficient α has a negative effect on the prey population, that is, the prey population decreases. When $\alpha = 3.54$, the system exhibits oscillations. In Figure 6, s varies from 0.01 to 0.18, and the results show that interspecific mortality s can change the stability of the system (1.2). It is found that when the competition coefficient s between predators increases to 0.18, the system exhibits a steady state. Further, Figure 7 shows that the increase in the value of the dependence coefficient m of the prey refuge ratio on the number of predators may be responsible for the stability of the system.

Next, in Figure 8, the bifurcation of the system (1.2) with respect to α is plotted.

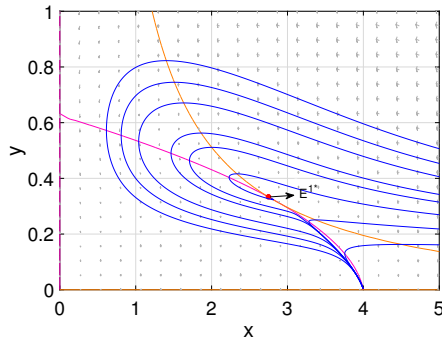


Figure 11. *
(a) $\alpha = 0.64$, $elk < d$

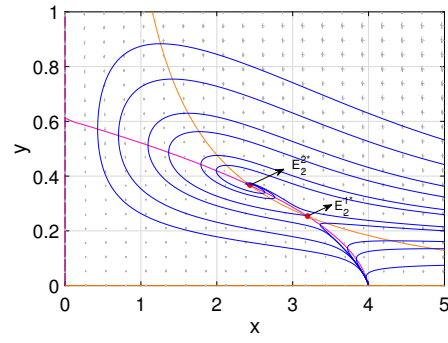


Figure 12. *
(b) $\alpha = 0.68$, $elk < d$

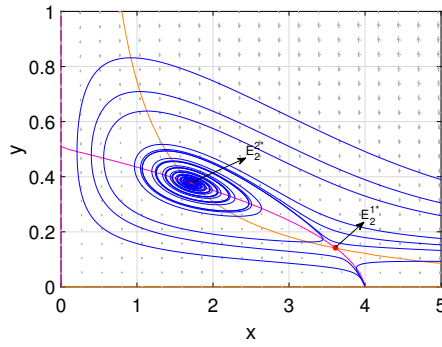


Figure 13. *
(c) $\alpha = 1$, $elk < d$

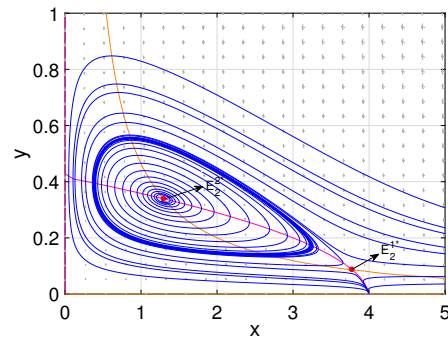


Figure 14. *
(d) $\alpha = 1.5$, $elk < d$

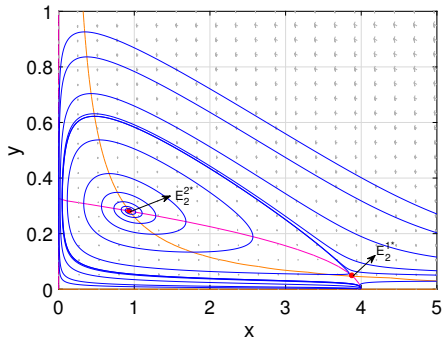


Figure 15. *
(e) $\alpha = 2.54$, $elk < d$

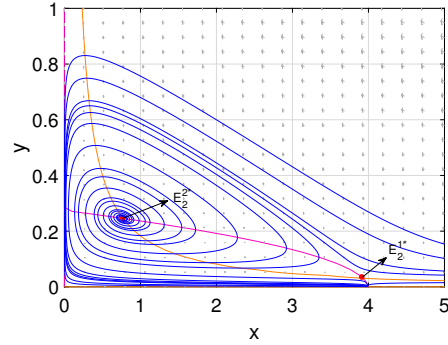


Figure 16. *
(f) $\alpha = 3.54$, $elk < d$

Figure 17. Phase diagram of equilibrium point stability at different values of cooperative hunting α . The other parameters are as follows: $r = 0.28$, $k = 4$, $l = 0.05$, $\theta = 0.26$, $m = 0.03$, $e = 0.18$, $d = 0.12$, $s = 0.03$.

In the bifurcation diagram, the blue solid curve represents a stable steady state, the red solid curve indicates instability, and the green region indicates the bifurcation of the periodic solution. It can be seen that if we change the value of α from 0.4 to 1.8, the system will undergo a Hopf bifurcation. The bifurcation diagram clearly shows that as the value of α increases, the number of prey decreases, while the number of predators rises first and then decreases. In addition, it is seen that a too large value of α destabilizes the system and leads to a Hopf bifurcation. Thus, we can conclude that an increase in cooperative hunting by predators can destabilize the system. On the other hand, Figure 9 shows the bifurcation diagram of system (1.2) with regard to s . The system experiences a Hopf bifurcation when the value of s is changed from 0 to 0.25, as seen in this diagram. Further, we observe that large values of s have the potential to stabilize the system, but values that are too large lead all the predators to extinction.

Bifurcation diagram of system (1.2) with respect to m has been drawn in Figure 10. From this figure, it is seen that if we change the value of m from 0 to 0.8, then the system possesses Hopf bifurcation. For $0 < m < 0.2314$ the system exhibits oscillating behavior, whereas for $0.2314 < m \leq 0.8$ the system exhibits stable steady state behavior. As a result, it may be concluded that the prey refuge ratio on the number of predators may be responsible for the stability of the system.

From the perspective of biology, cooperative predator hunting, prey refuge and interspecific competition are the key factors affecting dynamical behaviors of the prey-predator system. Initially, cooperative hunting is beneficial to the predator because the prey is less aware of refuge during this period, and the predator provides food for all cooperative members, so the number of predators grows. But with time, prey adopts the refuge behavior, and the predator can only successfully capture a certain quantity of prey. The predators' interspecific competition is heightened by this meager food supply. The predator will become an endangered species if this interspecific rivalry reaches its peak.

6. Conclusion

In the present study, we consider the dynamical behavior of inter-predator cooperation and prey population refuge. Firstly, we validate the positivity and boundedness of solutions of system (1.2). Secondly, the existence and stability of the system equilibrium points are analyzed in detail. Finally, theoretically, we study the sufficient conditions for Hopf bifurcation with respect to the dependence coefficient of the prey refuge ratio on the number of predators m in the system (1.2).

We have simulated the system (1.2) numerically by taking the values of the parameters. When the system parameters satisfy $elk < d$, the stability of the positive equilibrium point E_2^{2*} varies as the hunting cooperation coefficient α increases (see Figure 3). When $\alpha = 1.5$, the system will have a limit cycle, which disappears as α continues to increase. When the system parameters satisfy $elk > d$, it can be seen that the system has only one positive equilibrium point E_1^* . When the value of the hunting cooperative system α increases to 3.54, the system develops two limit cycles (see Figure 4). It is observed that as the predator-prey cooperation coefficient α increases, the system may be destabilized (see Figure 5, Figure 8). It is also found that the increase of interspecific competition coefficient s may stabilize the system (see Figure 6, Figure 9). It has been discovered that the increase in the value of the

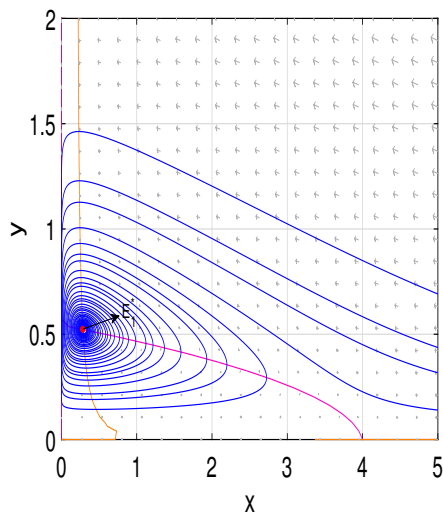


Figure 18. *
(a) $\alpha = 0.86$, $elk > d$

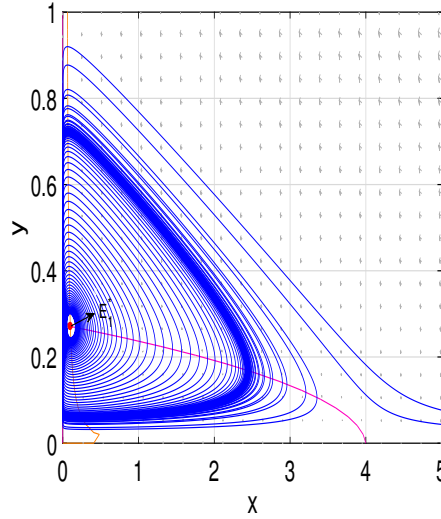


Figure 19. *
(b) $\alpha = 3.54$, $elk > d$

Figure 20. Phase diagram of the local stability of the system (1.2). For $\alpha = 0.86$, the system (1.2) has a unique positive equilibrium E_1^* , which is asymptotically stable; when the value of α increases to 3.54, two limit cycles appear in the system (1.2). The other parameters are as follows: $r = 0.28$, $k = 4$, $l = 0.05$, $\theta = 0.26$, $m = 0.03$, $e = 0.18$, $d = 0.01$, $s = 0.03$.

dependence coefficient m of the prey shelter ratio on the number of predators may be responsible for the stability of the system (see Figure 7, Figure 10). Therefore, by analyzing the system, we obtain the range of the control parameters α , s , and m that the predator-prey system can maintain.

Animals must engage in foraging to survive and reproduce. Different tactics are used by predators and prey to improve their density. To capture prey more effectively, predators cooperate in the hunting process. By cooperating in hunting to obtain animals that are larger or faster than themselves, they also increase their success rate in obtaining prey. As the rate of predator attack increases, prey populations defend themselves through refuge behavior. From a biological point of view, our study concludes that in the predator-prey system, predators follow cooperative hunting for food, while prey adopt a refuge behavior that is dependent on the predator to protect themselves from predators. These two factors play an important role in balancing the system. As prey species follow refuge behavior, predators are forced to use cooperation to capture more prey. It is due to the prey's refuge behavior that hunting food is in short supply, thus creating interspecific competition among predators. Predators will inevitably become extinct as this interspecific conflict intensifies, making them an endangered species. As a result, cooperative hunting and predator-dependent prey refuge are crucial to the stability of ecosystems.

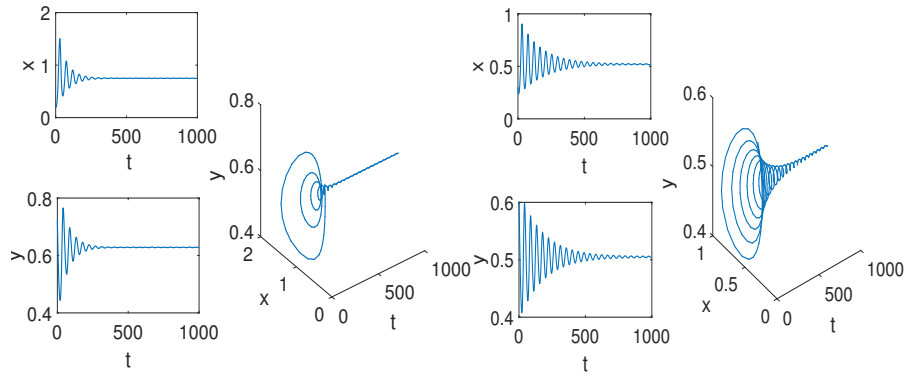


Figure 21. *
(a) $\alpha = 0.5$

Figure 22. *
(b) $\alpha = 0.86$

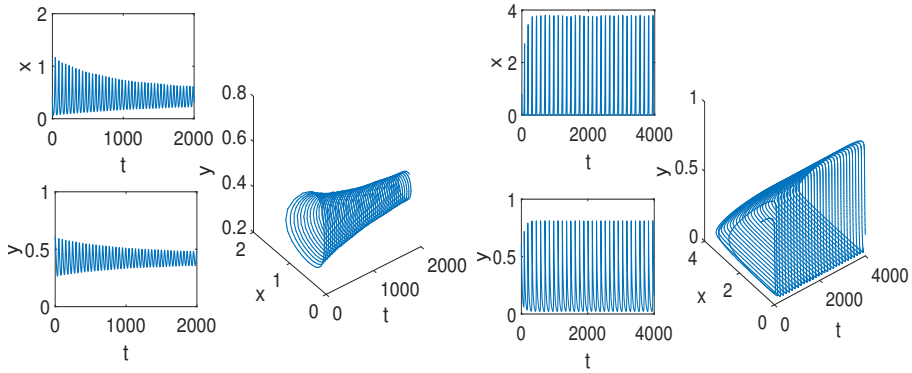


Figure 23. *
(c) $\alpha = 1.34$

Figure 24. *
(d) $\alpha = 3.54$

Figure 25. Time evolution, with parameters value $r = 0.28$, $k = 4$, $l = 0.05$, $\theta = 0.26$, $m = 0.03$, $e = 0.18$, $d = 0.03$, $s = 0.03$.

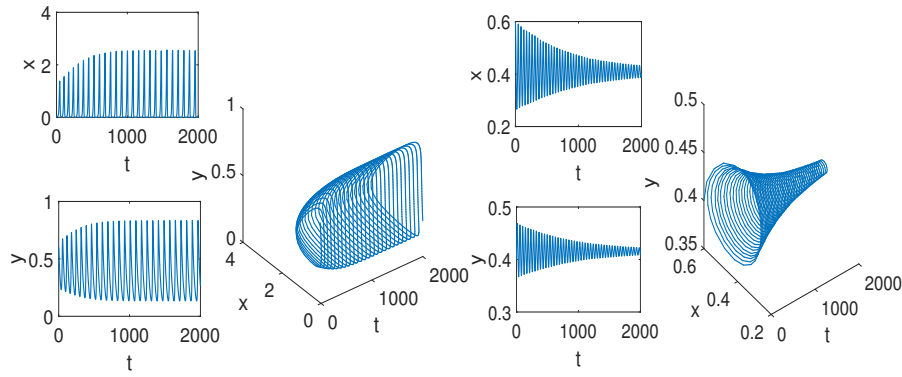


Figure 26. *
 $s = 0.01$

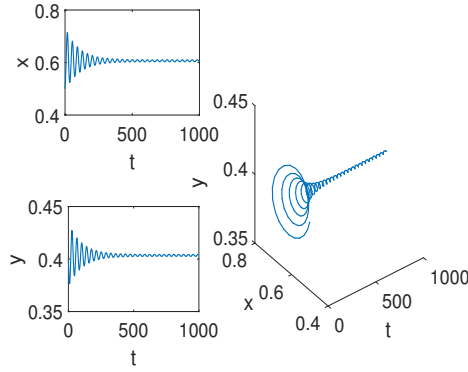


Figure 27. *
 $s = 0.035$

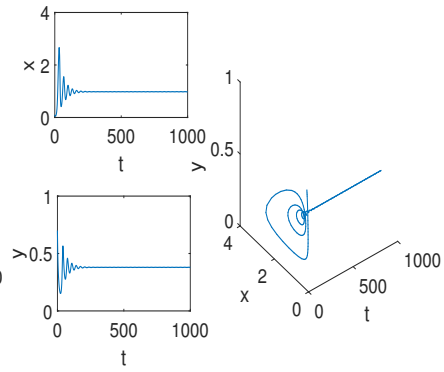


Figure 28. *
 $s = 0.085$

Figure 29. *
 $s = 0.18$

Figure 30. Time evolution, with parameters value $r = 0.28$, $k = 4$, $l = 0.05$, $\theta = 0.26$, $m = 0.03$, $e = 0.18$, $\alpha = 1.34$, $d = 0.03$.

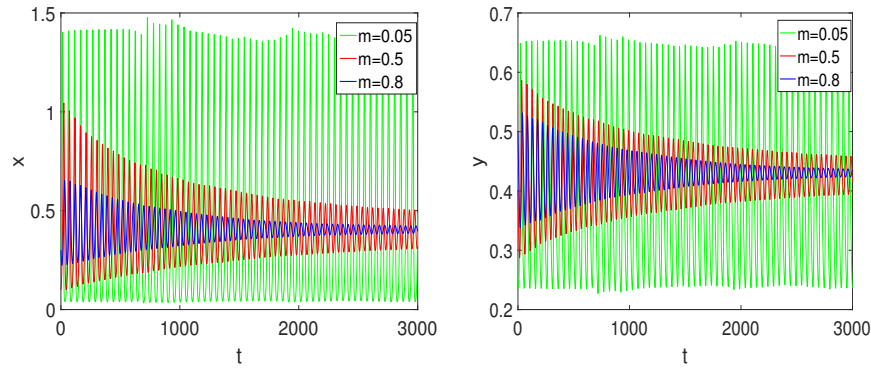


Figure 31. Figure shows time series solutions of the system (1.2). The other parameters are as follows: $r = 0.28$, $k = 4$, $l = 0.05$, $\theta = 0.26$, $s = 0.03$, $e = 0.19$, $\alpha = 1.34$, $d = 0.032$.

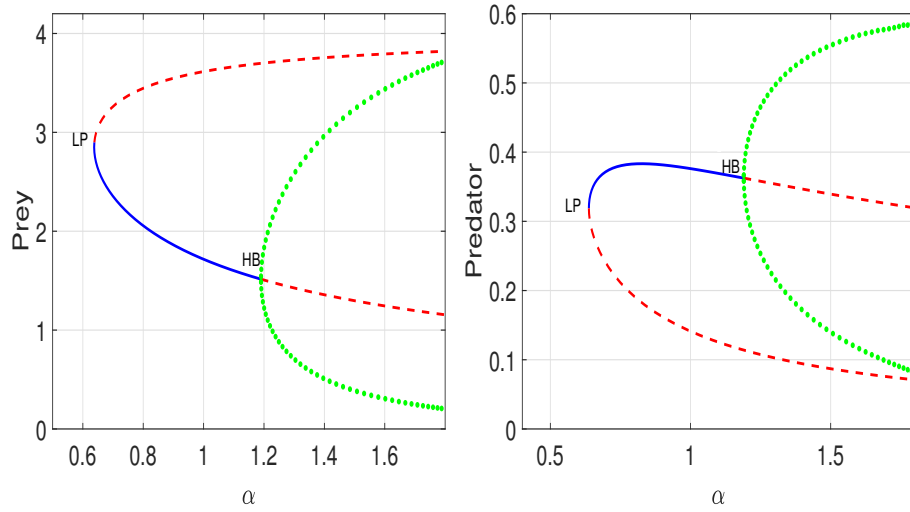


Figure 32. Bifurcation diagram of system (1.2) has been drawn with respect to α of prey and predator by taking the parametric values $r = 0.28$, $k = 4$, $l = 0.05$, $\theta = 0.26$, $m = 0.03$, $e = 0.18$, $d = 0.12$, $s = 0.03$.

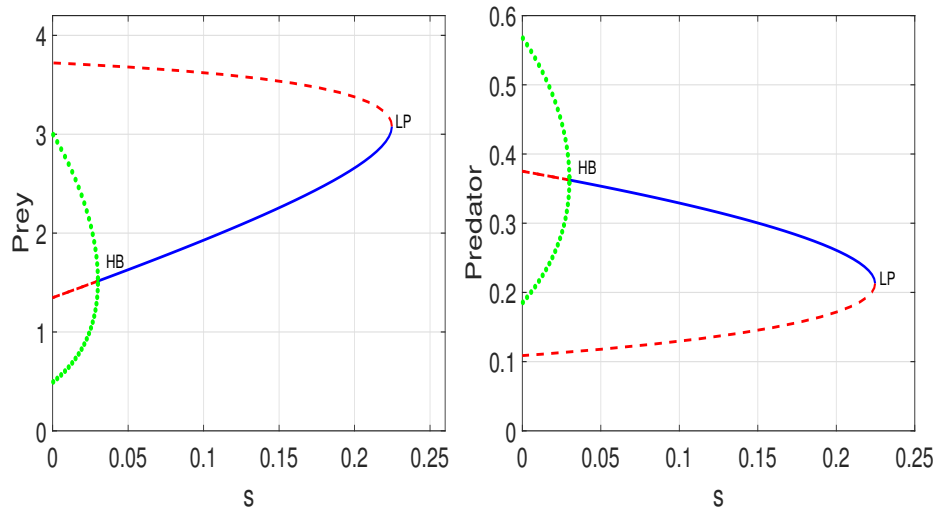


Figure 33. Bifurcation diagram of system (1.2) has been drawn with respect to s of prey and predator by taking the parametric values $r = 0.28$, $k = 4$, $l = 0.05$, $\theta = 0.26$, $m = 0.03$, $e = 0.18$, $d = 0.12$, $s = 0.03$.

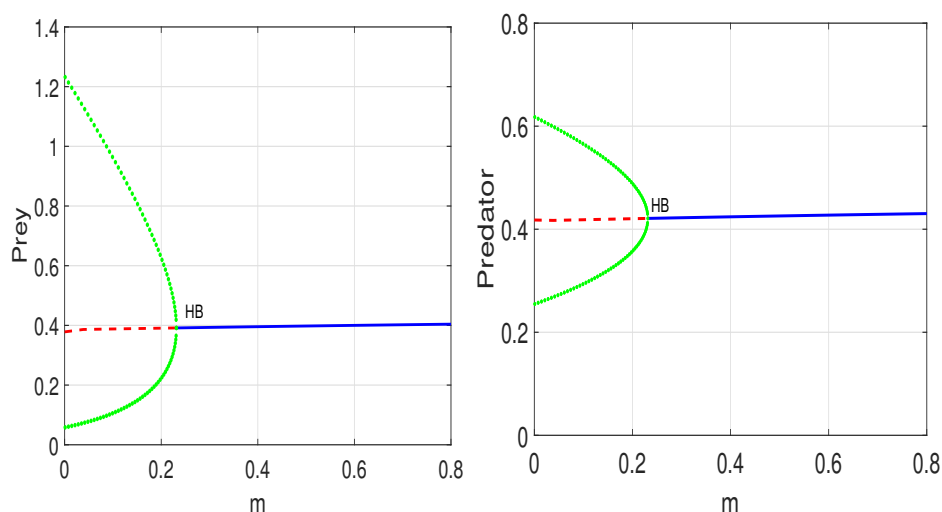


Figure 34. Bifurcation diagram of system (1.2) has been drawn with respect to m of prey and predator by taking the parametric values $r = 0.28$, $k = 4$, $l = 0.05$, $\theta = 0.26$, $\alpha = 1.34$, $e = 0.19$, $d = 0.032$, $s = 0.03$, $m = m_{hb} = 0.2314$.

Acknowledgements

The authors appreciate the reviewers and editors for their valuable suggestions that have greatly helped improve this paper.

References

- [1] D. Wu and M. Zhao, *Qualitative analysis for a diffusive predator-prey model with hunting cooperative*, Physica A: Statistical Mechanics and its Applications, 2019, 515, 299–309.
- [2] D. Song, C. Li and Y. Song, *Stability and cross-diffusion-driven instability in a diffusive predator-prey system with hunting cooperation functional response*, Nonlinear Analysis: Real World Applications, 2020, 54, 103106.
- [3] N. C. Pati, G. C. Layek, and Nikhil. Pal, *Bifurcations and organized structures in a predator-prey model with hunting cooperation*, Chaos, Solitons & Fractals, 2020, 140, 110184.
- [4] S. Fu and H. Zhang, *Effect of hunting cooperation on the dynamic behavior for a diffusive holling type II predator-prey model*, Communications in Nonlinear Science and Numerical Simulation, 2021, 99, 105807.
- [5] F. A. Rihan and H. J. Alsakaji, *Persistence and extinction for stochastic delay differential model of prey predator system with hunting cooperation in predators*, Advances in Difference Equations, 2020, 2020(1), 1-22.

- [6] V. Dinets, *Apparent coordination and collaboration in cooperatively hunting crocodilians*, *Ethology Ecology & Evolution*, 2015, 27(2), 244-250.
- [7] D. Scheel and C. Packer, *Group hunting behaviour of lions: a search for cooperation*, *Animal Behaviour*, 1991, 41(4), 697-709.
- [8] L. David. Mech, *The wolf: The ecology and behavior of an endangered species*, *Journal of Wildlife Management*, 1971, 52(3), 644-647.
- [9] A. L. Rypstra and R. S. Tirey, *Prey size, prey perishability and group foraging in a social spider*, *Oecologia*, 1991, 86(1), 25-30.
- [10] J. C. Bednarz, *Cooperative hunting harris' hawks (parabuteo unicinctus)*, *Science*, 1988, 239(4847), 1525-1527.
- [11] M. W. Moffett, *Foraging dynamics in the group-hunting myrmicine ant, *pheidologeton diversus**, *Journal of Insect Behavior*, 1988, 1(3), 309-331.
- [12] C. Cosner, D. L. DeAngelis, J. S. Ault and D. B. Olson, *Effects of spatial grouping on the functional response of predators*, *Theoretical Population Biology*, 1999, 56(1), 65-75.
- [13] L. Berec, *Impacts of foraging facilitation among predators on predator-prey dynamics*, *Theoretical Population Biology*, 2010, 72(1), 94-121.
- [14] M. T. Alves and F. M. Hilker, *Hunting cooperation and allee effects in predators*, *Journal of Theoretical Biology*, 2017, 419, 13-22.
- [15] S. R. J. Jang, W. Zhang and V. Larriva, *Cooperative hunting in a predator-prey system with allee effects in the prey*, *Natural Resource Modeling*, 2018, 31(4), e12194.
- [16] S. Pal, N. Pal, S. Samanta and J. Chattopadhyay, *Effect of hunting cooperation and fear in a predator-prey model*, *Ecological Complexity*, 2019, 39(8), 100770.
- [17] S. Halder, B. Joydeb, P. Samares and J. Bhattacharyya, *Comparative studies on a predator-prey model subjected to fear and allee effect with type I and type II foraging*, *Journal of Applied Mathematics and Computing*, 2020, 62, 93-118.
- [18] A. A. Thirthar, S. J. Majeed, M. A. Alqudah, P. Panja and T. Abdeljawad, *Fear effect in a predator-prey model with additional food, prey refuge and harvesting on super predator*, *Chaos Solitons & Fractals*, 2022, 159, 112091.
- [19] Y. Huang, F. Chen and Z. Li, *Stability analysis of a prey-predator model with holling type III response function incorporating a prey refuge*, *Applied Mathematics and Computation*, 2006, 182(1), 672-683.
- [20] G. D. Ruxton, *Short term refuge use and stability of predator-prey models*, *Theoretical Population Biology*, 1995, 47(1), 1-17.